

EXTRA COPY

NASA

LIBRARY COPY

MAR 3 1961

SPACE FLIGHT  
LANGLEY FIELD, VIRGINIA

# TECHNICAL NOTE

D-663

EXPERIMENTAL INVESTIGATION OF EFFECTS OF  
RANDOM LOADING ON THE FATIGUE LIFE OF NOTCHED CANTILEVER-  
BEAM SPECIMENS OF SAE 4130 NORMALIZED STEEL

By Robert W. Fralich

Langley Research Center  
Langley Field, Va.

NATIONAL AERONAUTICS AND SPACE ADMINISTRATION  
WASHINGTON

February 1961

## NATIONAL AERONAUTICS AND SPACE ADMINISTRATION

## TECHNICAL NOTE D-663

EXPERIMENTAL INVESTIGATION OF EFFECTS OF  
RANDOM LOADING ON THE FATIGUE LIFE OF NOTCHED CANTILEVER-  
BEAM SPECIMENS OF SAE 4130 NORMALIZED STEEL

By Robert W. Fralich

## SUMMARY

Results of random-loading fatigue tests on 145 notched cantilever-beam specimens and constant-amplitude fatigue tests on 75 similar specimens are presented. The fatigue lives for the two sets of results are compared at equal root-mean-square values of peak stresses. Compared on this basis, fatigue life was shorter for the random loading than for the constant-amplitude loading. A comparison of the random-loading results is also made with theoretical results which are based on the assumption of linear cumulative fatigue damage. The theoretical results overestimate the fatigue life over the range of stresses considered.

## INTRODUCTION

Fatigue failure of structural components subjected to random loadings represents one of the critical problems encountered in high-performance aircraft and missiles. Random loadings encountered may include gust loads, buffeting loads, runway-roughness loads, and acoustic loads in the noise fields of jet and rocket engines. These types of loading are characterized by continuous frequency spectrums, and such loadings may produce a repetition of stress peaks of sufficient magnitude to cause fatigue damage. There is particular danger of fatigue failure if the structural characteristics are such that a natural frequency occurs in a region where the loading spectrum has appreciable magnitude.

In the past, several experimental investigations have been conducted under loading schedules which are simplified approximations to the loading histories of various random loadings. (See, for example, refs. 1 to 8.) Actual random loadings were used in the experimental investigations of references 9 and 10, in which the fatigue properties under random and constant-amplitude loadings were investigated and compared for 2024-T3

and 7075-T6 aluminum alloys, respectively. In these investigations notched cantilever beams were tested in bending by applying the load at the tip. These papers also present calculated theoretical results for random loading based upon Miner's rule for cumulative damage (ref. 11). In the present paper results of a similar experimental investigation are presented for SAE 4130 steel specimens along with the calculated result for random loading. The equipment and test procedure used for the experimental investigation and the method of calculation of theoretical results were the same as those used in reference 10.

### SYMBOLS

$f_o$	resonant frequency of system, cps
$n$	number of cycles at a given stress level
$N$	number of cycles to failure
$R$	radius
$t_f$	time to failure, sec
$\sigma$	stress, psi or ksi
$\sigma_p$	peak stress, psi or ksi

### EXPERIMENTAL INVESTIGATION

#### Specimens

The notched cantilever specimens used in this investigation were machined according to the dimensions shown in figure 1. The dimensions shown here are nominal; the actual dimensions used for computing section properties were measured for each specimen to the nearest 0.001 inch before testing. The notched configuration corresponds to a theoretical elastic stress-concentration factor of 7.25 for an axially loaded specimen.

The specimens were machined from 3/16-inch SAE 4130 normalized steel sheets. A light surface grinding in the longitudinal direction was used on the top and bottom surfaces after machining in order to remove sheet surface imperfections. Metallurgical examination indicated that the longitudinal axis of the specimen was transverse to the direction of rolling of the sheets.

## Test Equipment and Procedure

Random loading.-- The equipment and test procedure employed in reference 10 was used for the present random-loading fatigue investigation. A schematic diagram of the equipment is shown in figure 2.

The random force applied to the specimen in these tests was obtained from a tape recording of the noise produced by a 2-inch subsonic cold air jet. The recording consisted of repetitions of a 6.4-second sample of the noise. In this recording, the force signal was recorded by a frequency modulation system so that wear of the magnetic tape would not affect the magnitude of the force applied to the specimen. Although the cold air jet was used to obtain the random-force signal, an equivalent power spectrum of stress response could have been obtained from other types of random-force inputs provided that they had reasonably flat spectra in the vicinity of the natural frequency of the specimen configuration and no large peaks in the other frequency ranges.

The equipment used to apply the random force to the specimen is shown in figure 2(a). In this equipment the force signal, obtained by demodulation of the playback of the frequency-modulated tape recording, was amplified and fed into an electromagnetic shaker which applied the load to the specimen. The amplification of the force signal was controlled at the amplifier. A timer was included in the circuit to measure the time to failure.

The equipment shown in figure 2(b) was used to measure and record the current in the shaker drive coil (proportional to the force applied to the shaker drive coil) and the output of a strain gage mounted on the specimen. These force and strain signals were amplified and read on a root-mean-square thermocouple meter and were also recorded on magnetic tape. Provision was also made to apply a known calibration signal to the meter and tape recorder. A cathode-ray oscillograph was used to monitor the force and strain signals.

Each specimen was clamped in support blocks, between plastic shims, which were inserted to relieve effects of stress concentration at the grip. (See figs. 1 and 3.) The shaker drive coil was connected to the tip of the specimen by a flexible connector which eliminated torsional and longitudinal loads. (See fig. 3.) The fundamental natural frequency of the specimen with the shaker attached was about 123 cps.

In this part of the investigation, 145 specimens were tested to failure at various levels of root-mean-square stress. For the type of loading applied in this investigation the mean stress is zero. At the start of the test on each specimen, the root-mean-square value of force was adjusted to give the desired root-mean-square value of stress and was held constant during the remainder of the test. At the start of each test,

45-second samples of the force and stress signals were recorded on magnetic tape and the root-mean-square values were read. The test was continued until complete failure of the specimen took place. The time to failure was then recorded.

Constant-amplitude loading.- For the experimental investigation with constant-amplitude loading, the load was applied sinusoidally at 30 cps by the cantilever-sheet bending machine described in reference 10 and shown in figure 4. As in the random-load tests, plastic shims were used in the grips, and the machine attachment prevented the application of torsional and longitudinal loads to the specimen. The root-mean-square value of the strain-gage output was measured with the equipment illustrated in figure 2(b).

Tests were performed on 75 specimens at various stress amplitudes and zero mean stress. Each specimen was tested to failure at a constant value of stress amplitude.

#### Calculation of Stresses From Measured Strains

The stress in each specimen was obtained from the output of a wire-resistance strain gage mounted at the notched section of the specimen. (See fig. 1.) As in reference 10, the specimen was statically calibrated to obtain a static stress-calibration factor which relates the strain-gage-bridge output to the calculated surface bending stress at the notched cross section. The surface bending stress was based on beam properties at the notch and the effect of stress concentration was neglected in the calculation. For the fatigue tests, the stress calibration factor was used to obtain root-mean-square values of nominal stress from the measured root-mean-square value of the bridge output.

### RESULTS AND DISCUSSION

#### Stress Response for Random Loading

The characteristics of the force input and stress output are shown in figure 5. One-second records of the force and stress histories are shown in figure 5(a) for a specimen tested at a root-mean-square stress of 7,800 psi. The force shown in this figure is the input force applied to the vibrating system, that is, the force applied to the shaker drive coil. The corresponding power spectra are shown in figure 5(b) for the force signal and in figure 5(c) for the stress signal; the magnitudes are given on logarithmic vertical scales.

The power spectrum of the stress response presented in figure 5(c) shows that the specimen responds only to frequency components near its own natural frequency, even though the power spectrum of the force input covered a much wider frequency range. (See fig. 5(b).) This fact is also observed from the stress history of figure 5(a), in which the stress has essentially a constant frequency and a variable amplitude. The stress thus represents the response of a lightly damped vibrating system to a force input which has a reasonably flat spectrum in the vicinity of the natural frequency of the vibrating system and no large peaks in the other frequency ranges.

In order to check the probability distribution of the stress, an electronic counter was used to count the number of times in 10 seconds that the stress crossed various thresholds of stress with positive slope. For example, the results for two root-mean-square stress levels are given by the test points of figure 6. Each test point represents the average of five readings and gives the average number of times per second that the stress passes through the value given by the abscissa with positive slope. For the higher root-mean-square stress level the fatigue life was too short for the measurements to be made on the stress signal itself; therefore, these measured values were obtained from the magnetic recording of the stress signal. For a stress response of a lightly damped vibrating system to a flat spectrum of force input in which the process is Gaussian, the curve of figure 6 shows the expected number of times per second that the stress will pass through a given value with positive slope. The experimental results agree well with the curve for a Gaussian distribution; therefore, the probability distribution of the stress for the experimental results was considered to be nearly Gaussian.

### Test Results

The results for the 145 random-loading tests are given in figure 7 in terms of the quantities measured in the test, that is, the root-mean-square nominal stress and the time to failure. Fatigue life is also indicated in terms of an equivalent number of cycles to failure, obtained by multiplying the time to failure by the natural frequency (123 cps). Also shown in this figure is a mean curve drawn through the test points.

The results of the 75 constant-amplitude-loading tests are given in figure 8, in which the fatigue life is shown as a function of nominal stress amplitude. Fatigue life is shown in terms of the number of cycles of stress reversals for failure and also in terms of an equivalent time to failure, which is the quotient of the number of cycles and the natural frequency (123 cps). The solid curve on this figure is a mean curve drawn through the test points. The maximum stresses were limited by the capacity of the testing machine; however, information at the higher stress levels was needed for use in theoretical calculations. The extrapolated

portion of the curve of figure 8 was guided by fatigue results of other notched specimens of 4130 normalized steel (for example, ref. 12).

In both sets of tests, the fatigue cracks originated at the corners of the cross section and grew inwardly until complete failure of the specimen. There were indications of the initiation of cracks before half the total time to failure.

### Theoretical Results

The stresses in the present random-loading investigation consist of the response of a lightly damped vibration system to a random loading that has a reasonably flat frequency spectrum which encompasses a natural frequency of the system. A method for the calculation of the probable time to failure was presented in reference 10. In this method, based on the theory of reference 13, the assumption is made that Miner's rule (ref. 11) for linear cumulative damage applies. The probable time to failure  $t_f$  is given by the following equation as a function of the root-mean-square value of the peak stresses  $\sqrt{\sigma_p^2}$ :

$$t_f = \left[ \frac{2f_0}{\sigma_p^2} \int_0^\infty \frac{\sigma e^{-\left(\sigma/\sqrt{\sigma_p^2}\right)^2}}{N(\sigma)} d\sigma \right]^{-1} \quad (1)$$

in which

$$\sqrt{\sigma_p^2} = \sqrt{2\sigma^2} \quad (2)$$

In these equations  $f_0$  is the resonant frequency of the vibrating system,  $N(\sigma)$  is the number of cycles to failure for stress reversals with an amplitude  $\sigma$ , and  $\sqrt{\sigma^2}$  is the root-mean-square stress. The probable time to failure is expressed in terms of the root-mean-square value of the peak stresses instead of the root-mean-square stress, since the fatigue damage of a cycle of stress is generally considered to depend on stress amplitude rather than on the shape of the stress cycle.

For the configuration under consideration in this investigation,  $f_0 = 123$  cps and  $N(\sigma)$  is obtained from the mean S-N curve of figure 8. Equation (1) is integrated numerically for the probable time to failure for various values of  $\sqrt{\sigma_p^2}$ . These results are shown by the long- and short-dashed curve of figure 9.

## Comparison of Results

A summary of the fatigue results obtained in this investigation is given in figure 9, where the root-mean-square value of the peak nominal bending stresses is plotted against fatigue life. It should be recalled that the nominal bending stress ignores the effects of stress concentration. Furthermore, the root-mean-square value of the peak stresses for constant-amplitude loading corresponds to the actual peak value and, for random loading, is  $\sqrt{2}$  times the root-mean-square stress level. (See eq. (2).) Fatigue life is indicated both by time to failure and number of cycles to failure.

The solid-line curve is the mean curve through the experimental results of figure 7 for random loading; the dashed-line curve is the mean curve through the experimental results of figure 8 for constant-amplitude loading; and the long- and short-dashed curve shows the theoretical results for random loading.

Comparison of the curves for random loading and for constant-amplitude loading shows that, when compared on the basis of the root-mean-square value of the peak stresses, the two types of loading do not give equivalent fatigue lives but that random loading gives a shorter fatigue life than constant-amplitude loading. One reason for this result, especially at the lower stress levels, is the fact that the root-mean-square value of the stress peaks for random loading contains the effect of stress cycles which are below the fatigue limit but which do not appreciably affect the fatigue life of the specimen.

Comparison of the theoretical curve with the random-loading curve shows that the calculated fatigue life overestimates the fatigue life over the range of stress levels considered. The ratio of predicted to the experimentally obtained fatigue life is between 1.3 and 2.0 for the considered stress levels above  $\sqrt{\sigma_p^2} = 10$  ksi and increases as the stress level is decreased below 10 ksi. A similar trend for values of the ratio was found in reference 9 for 2024-T4 aluminum alloy, but a different trend was observed in reference 10 for 7075-T6 aluminum alloy in which the ratio is less than unity for the high stress levels and approaches unity for the lower stress values. Since the theoretical results were obtained by use of Miner's rule for cumulative damage, the comparison between experimental and theoretical results can also be given

in terms of the summation of cycle ratios  $\sum \frac{n}{N}$ , in which  $n$  is the number of cycles applied at a given stress level and  $N$  is the number of cycles to failure at this level. The reciprocal of the ratio of the predicted to the experimentally obtained fatigue life is equivalent

to  $\sum \frac{n}{N}$  and thus for the present investigation  $\sum \frac{n}{N} < 1$ . These results are in agreement with the results of several investigations in which variable-amplitude fatigue tests were performed at zero mean stress under various programs of loading which approximate various random loadings. In each of these investigations  $\sum \frac{n}{N}$  was found to be less than unity for the majority of tests performed. The materials included in these investigations were ASTM designation A-7 steel (ref. 3), SAE 4340 steel (ref. 7), 2024 aluminum alloy (refs. 2, 5, 6, and 7), and 7075 aluminum alloy (refs. 2, 4, and 5).

### CONCLUSIONS

Fatigue tests were made on 145 notched cantilever-beam specimens of SAE 4130 normalized steel under random loading. Results were also obtained for 75 similar specimens under constant-amplitude loadings. Comparison of the two sets of results on the basis of root-mean-square value of the peak nominal stress shows that the two types of loading do not give equivalent fatigue lives but that random loading produces fatigue failure in a shorter time. A theoretical calculation based on Miner's cumulative damage criterion overestimated the fatigue life over the range of stresses considered. In previous random-load investigations, a similar result had been found for 2024-T4 aluminum alloy but a different result had been found for 7075-T6 aluminum alloy in which the calculated time to failure underestimated the time to failure at the high stress levels and predicted the time to failure fairly well at the low stress levels. Comparison between the experimental and the theoretical results was made on the basis of  $\sum \frac{n}{N}$ , where  $n$  is the number of cycles at a given stress level and  $N$  the number of cycles to failure. This comparison shows that  $\sum \frac{n}{N} < 1$  for the present investigation is in agreement with the results of several fatigue investigations of various materials under programmed stresses of variable-amplitude and zero mean stress.

Langley Research Center,  
National Aeronautics and Space Administration,  
Langley Field, Va., November 25, 1960.

## REFERENCES

1. Dolan, T. J., Richart, F. E., Jr., and Work, C. E.: The Influence of Fluctuations in Stress Amplitude on the Fatigue of Metals. Proc. ASTM, vol. 49, 1949, pp. 646-679.
2. Freudenthal, A. M., Heller, R. A., and O'Leary, P. J.: Cumulative Fatigue Damage of Aircraft Structural Materials - Part 1: 2024 and 7075 Aluminum Alloy. WADC Tech. Note 55-273, Pt. 1, U.S. Air Force, June 1955.
3. Munse, W. H., Fuller, James R., and Petersen, Kenneth S.: Cumulative Damage in Structural Joints. Bull. 544, Am. Railway Eng. Assoc., June-July 1958, pp. 67-128.
4. Hardrath, Herbert F., Utley, Elmer C., and Guthrie, David E.: Rotating-Beam Fatigue Tests of Notched and Unnotched 7075-T6 Aluminum-Alloy Specimens Under Stresses of Constant and Varying Amplitudes. NASA TN D-210, 1959.
5. Naumann, Eugene C., Hardrath, Herbert F., and Guthrie, David E.: Axial-Load Fatigue Tests of 2024-T3 and 7075-T6 Aluminum-Alloy Sheet Specimens Under Constant- and Variable-Amplitude Loads. NASA TN D-212, 1959.
6. Hardrath, Herbert F. and Utley, Elmer C., Jr.: An Experimental Investigation of the Behavior of 24S-T4 Aluminum Alloy Subjected to Repeated Stresses of Constant and Varying Amplitudes. NACA TN 2798, 1952.
7. Freudenthal, Alfred M., and Heller, Robert A.: On Stress Interaction in Fatigue and a Cumulative Damage Rule - Part I. 2024 Aluminum and SAE 4340 Steel Alloys. WADC Tech. Rep. 58-69, Pt. I, ASTIA Doc. No. 155687, U.S. Air Force, June 1958.
8. Liu, H. W. and Corten, H. T.: Fatigue Damage During Complex Stress Histories. NASA TN D-256, 1959.
9. Head, A. K., and Hooke, F. H.: Random Noise Fatigue Testing. Proc. Int. Conf. on Fatigue of Metals (London and New York), Inst. Mech. Eng. and A.S.M.E., 1956, pp. 301-303.
10. Fralich, Robert W.: Experimental Investigation of Effects of Random Loading on the Fatigue Life of Notched Cantilever-Beam Specimens of 7075-T6 Aluminum Alloy. NASA MEMO 4-12-59L, 1959.

11. Miner, Milton A.: Cumulative Damage in Fatigue. Jour. Appl. Mech., vol. 12, no. 3, Sept. 1945, pp. A-59 - A-164.
12. Illg, Walter: Fatigue Tests on Notched and Unnotched Sheet Specimens of 2024-T3 and 7075-T6 Aluminum Alloys and of SAE 4130 Steel with Special Consideration of the Life Range from 2 to 10,000 Cycles. NACA TN 3866, 1956.
13. Miles, John W.: An Approach to the Buffeting of Aircraft Structures by Jets. Rep. No. SM-14795, Douglas Aircraft Co., Inc., June 1953.

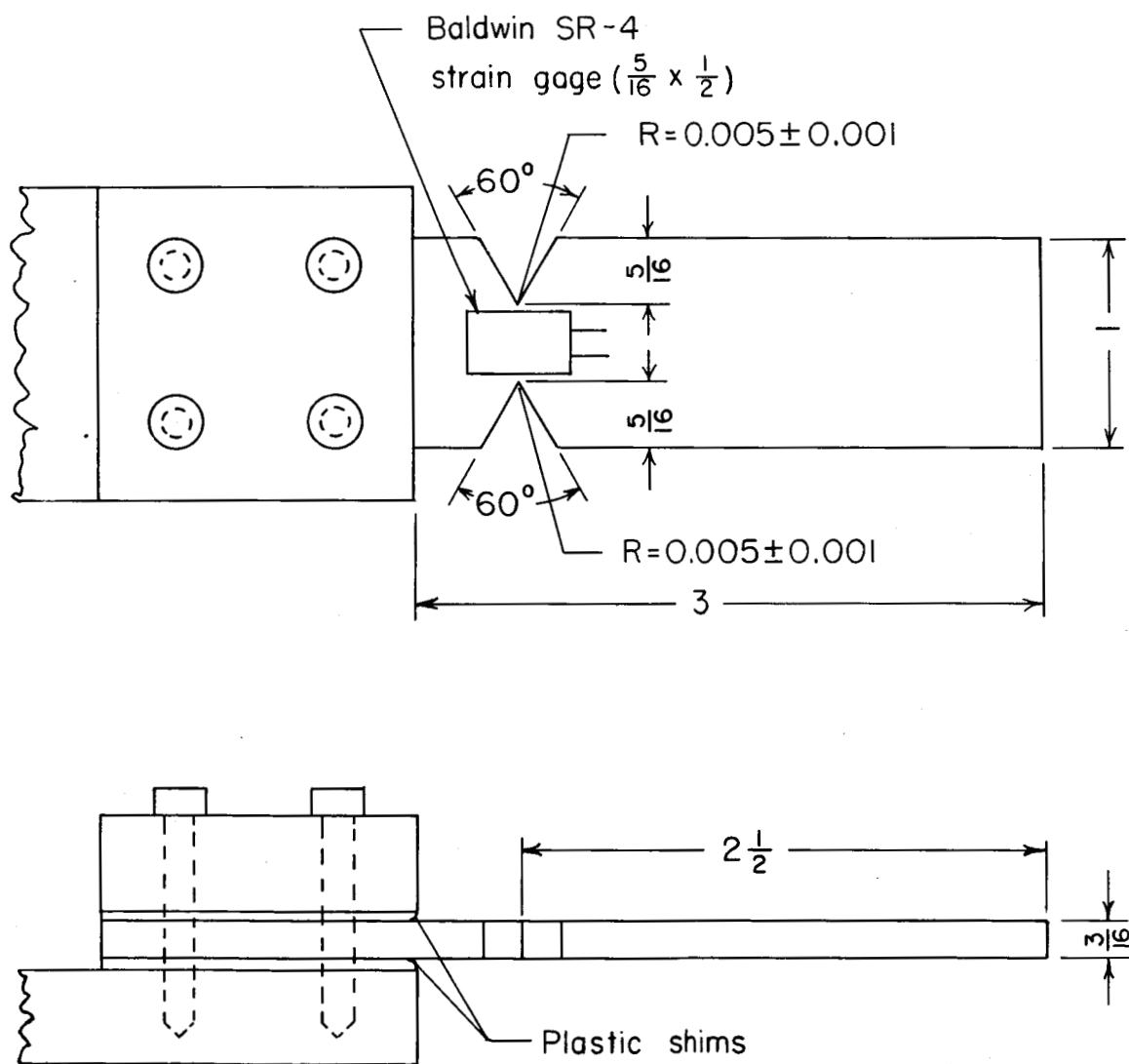
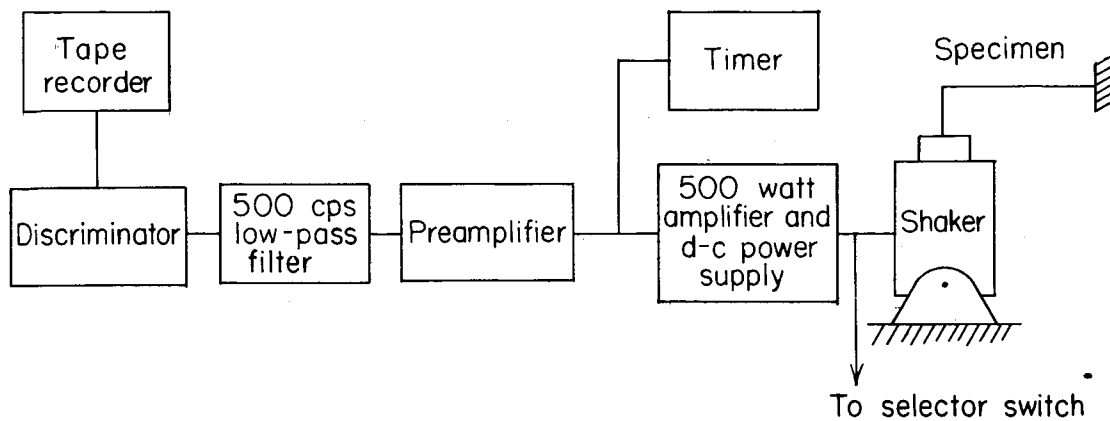
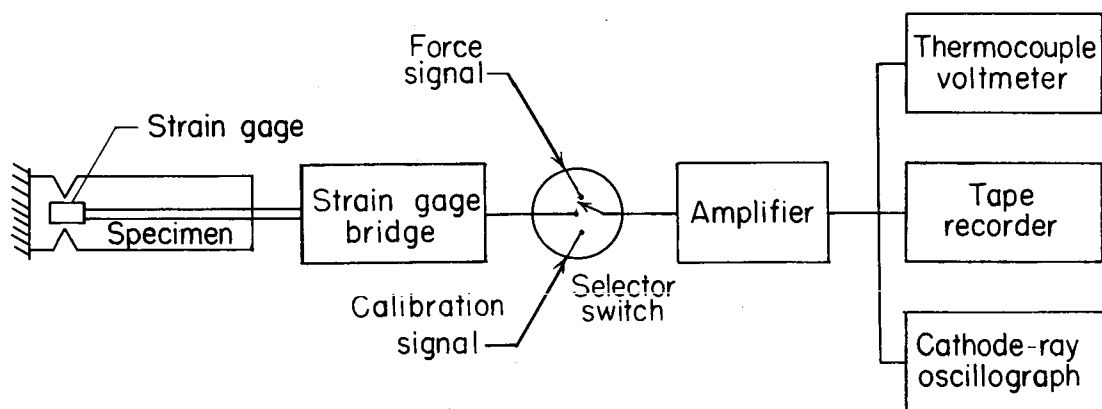


Figure 1.- Test specimen. All dimensions are in inches.

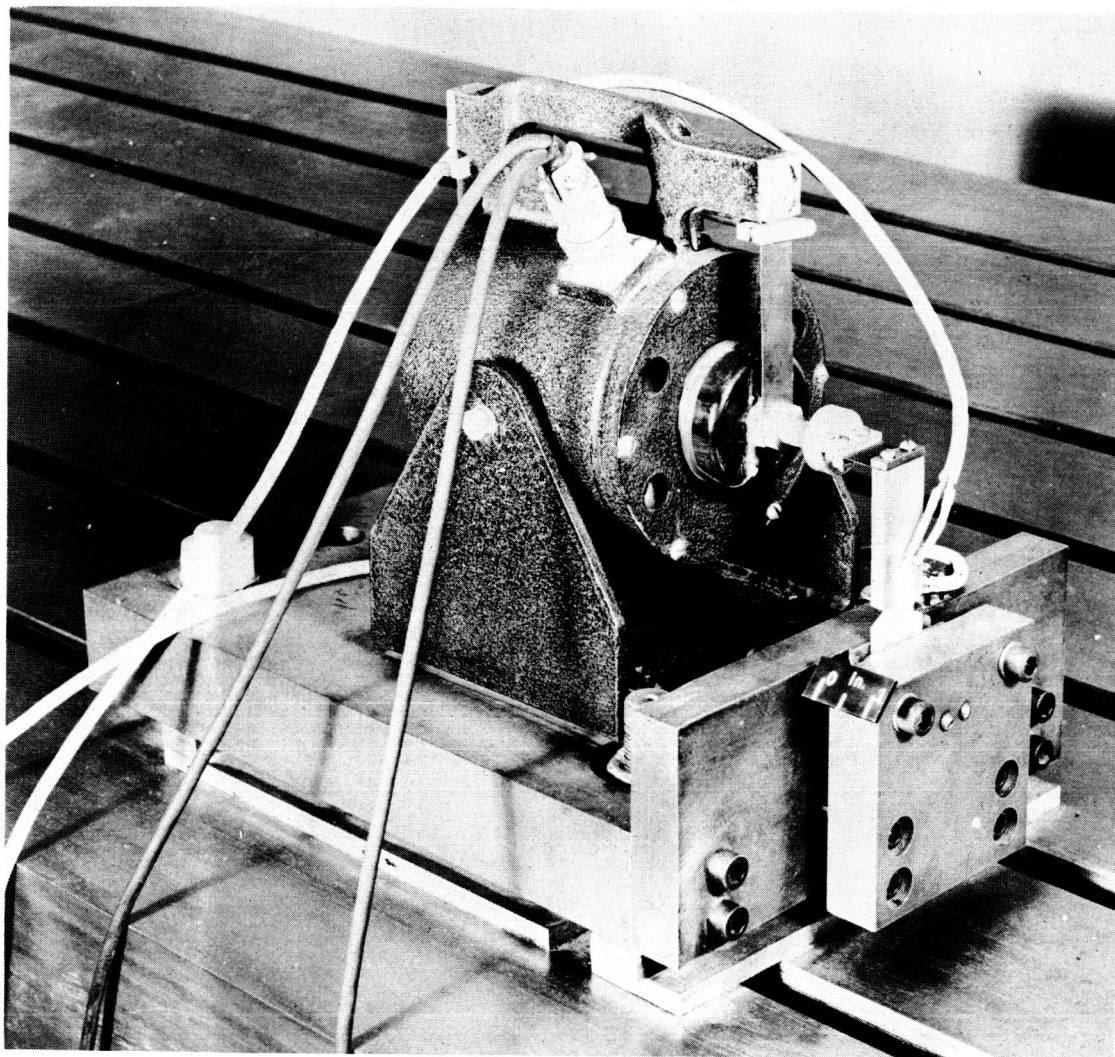


(a) Force-application equipment.



(b) Data-measuring equipment.

Figure 2.- Schematic diagram of test equipment.



L-57-4373

Figure 3.- Specimen mounted in shaker for random-loading tests.

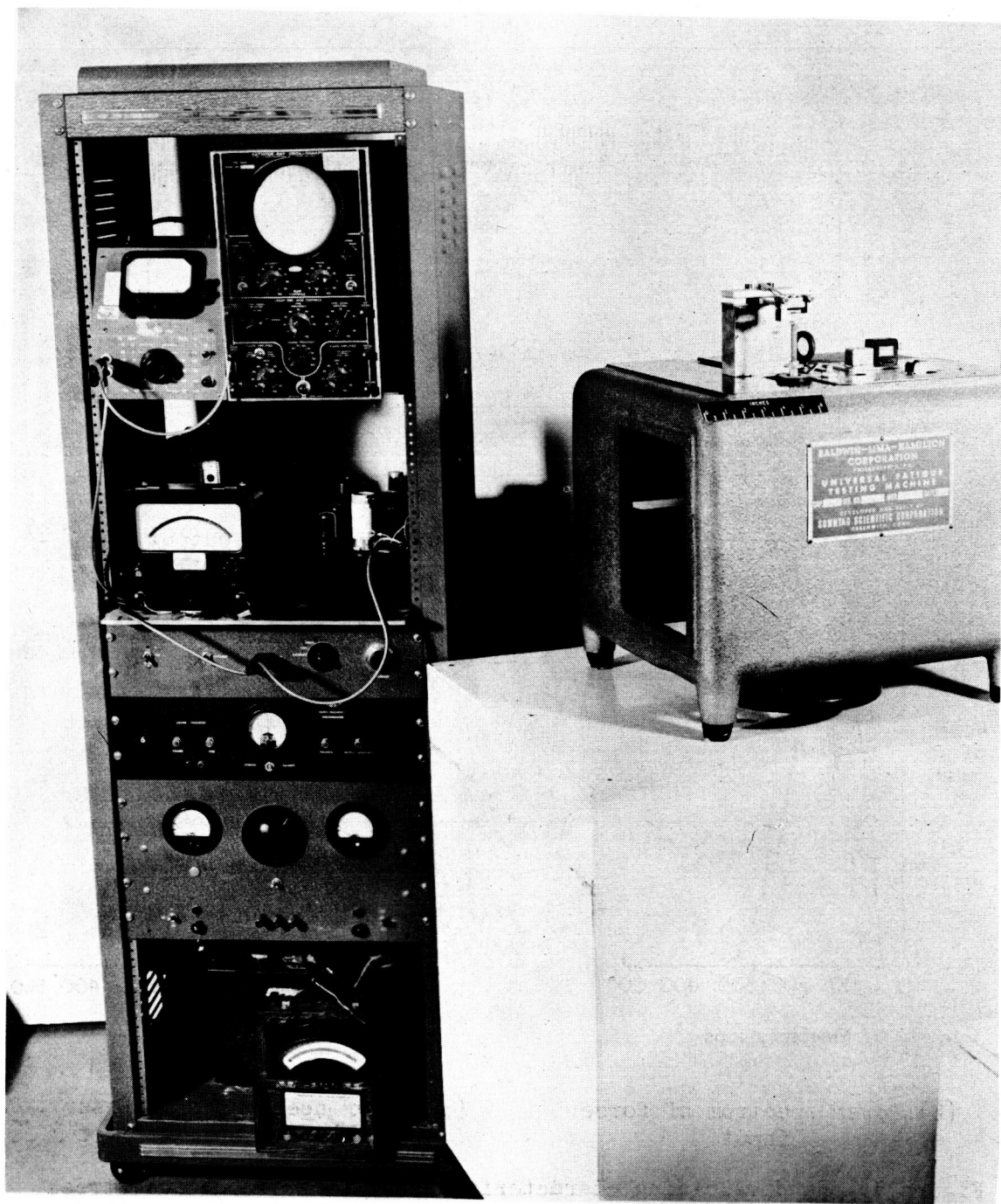
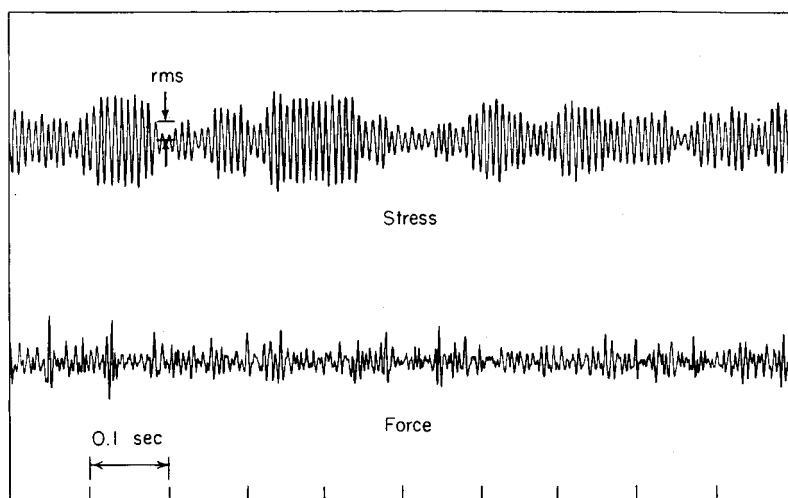
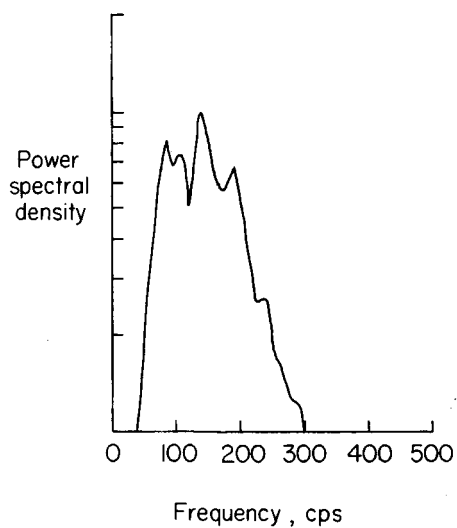


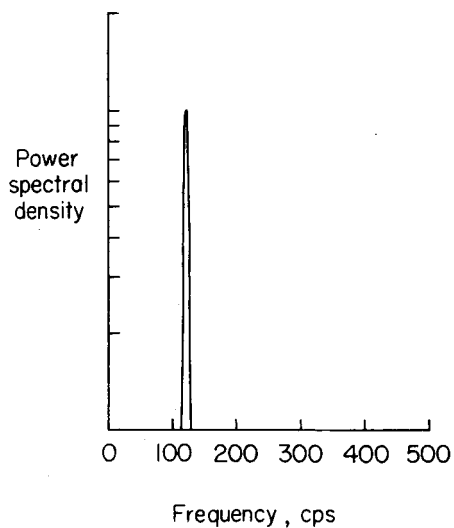
Figure 4.- Constant-amplitude loading equipment. L-57-4374



(a) Time histories of force input and stress output.



(b) Power spectrum of force input.



(c) Power spectrum of stress output.

Figure 5.- Random-loading characteristics of force input and stress output for a typical specimen.

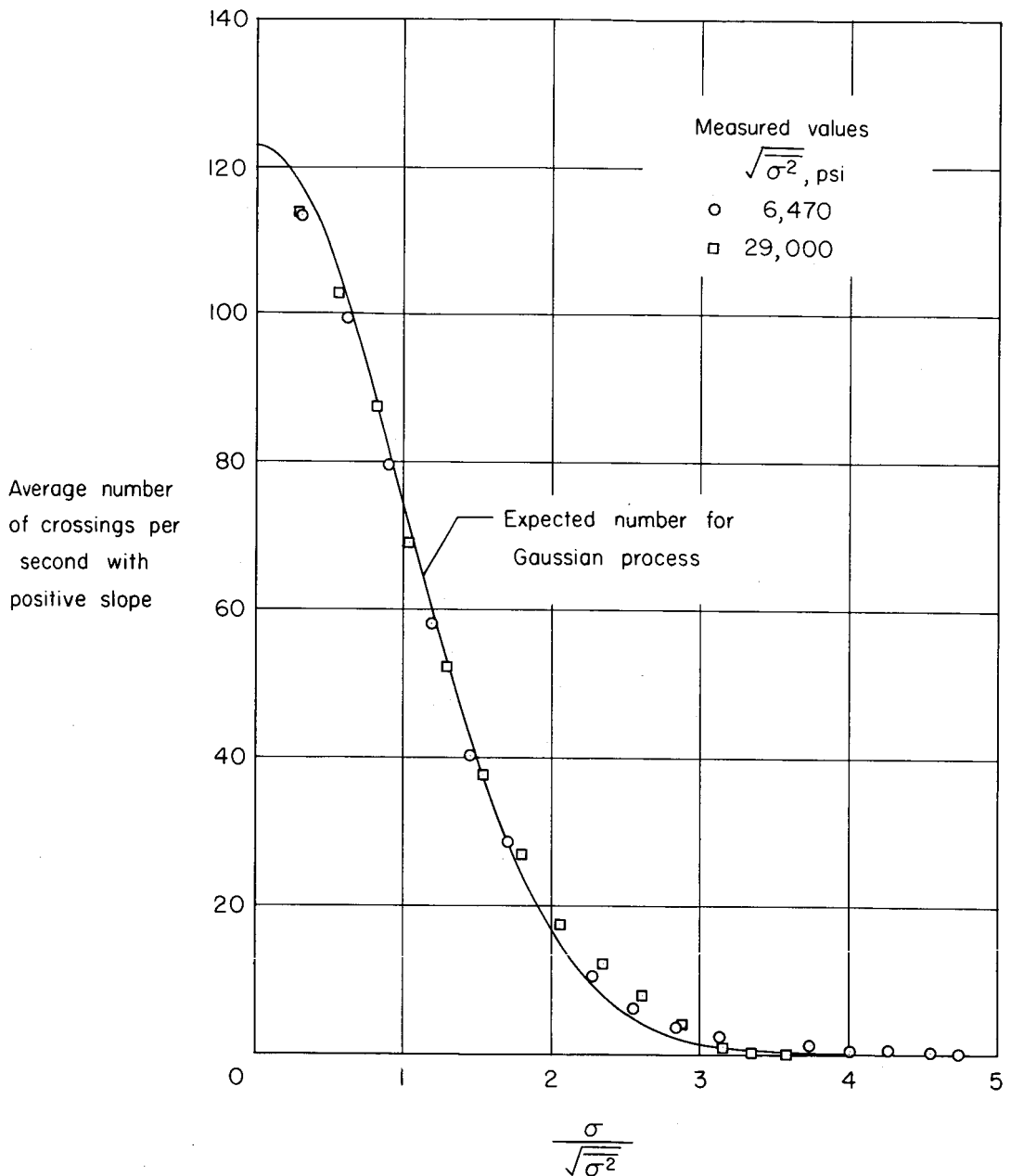


Figure 6.- Average number of times per second that the stress crosses the stress level  $\sigma$  with positive slope for two values of root-mean-square stress  $\sqrt{\sigma^2}$ . (Measured values obtained from strain signal for  $\sqrt{\sigma^2} = 6,470$  psi and from playback of magnetic recording of strain signal for  $\sqrt{\sigma^2} = 29,000$  psi.)

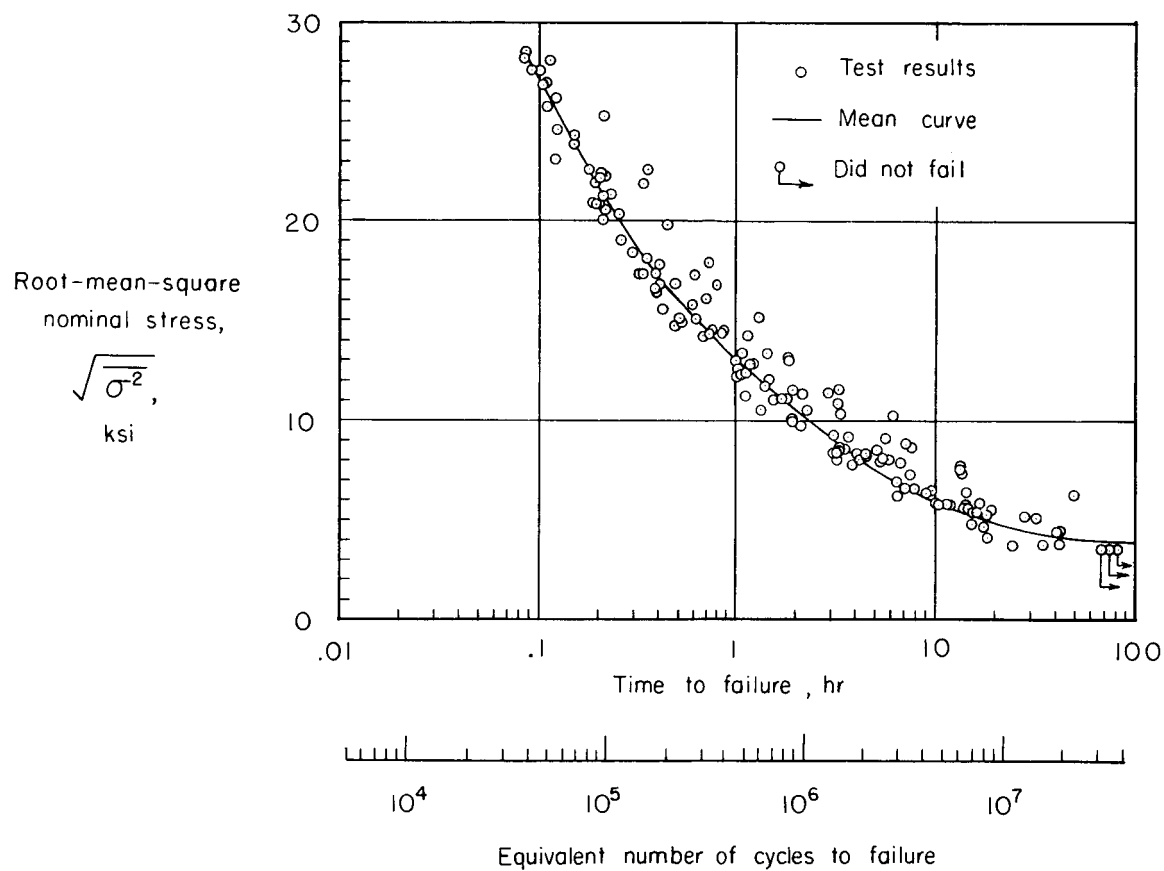


Figure 7.- Fatigue results of random-loading tests.

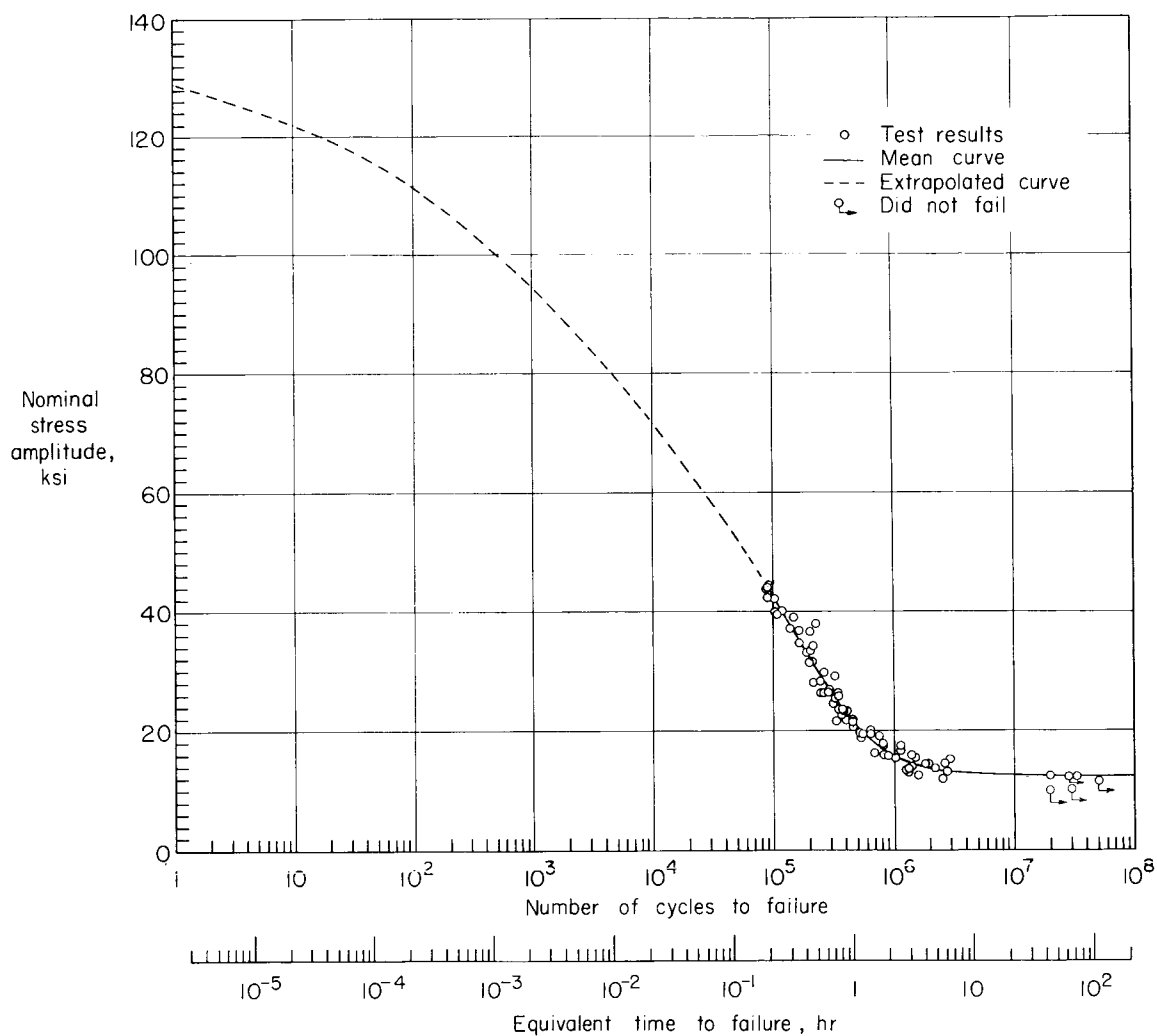


Figure 8.- Fatigue results of constant-amplitude-loading tests.

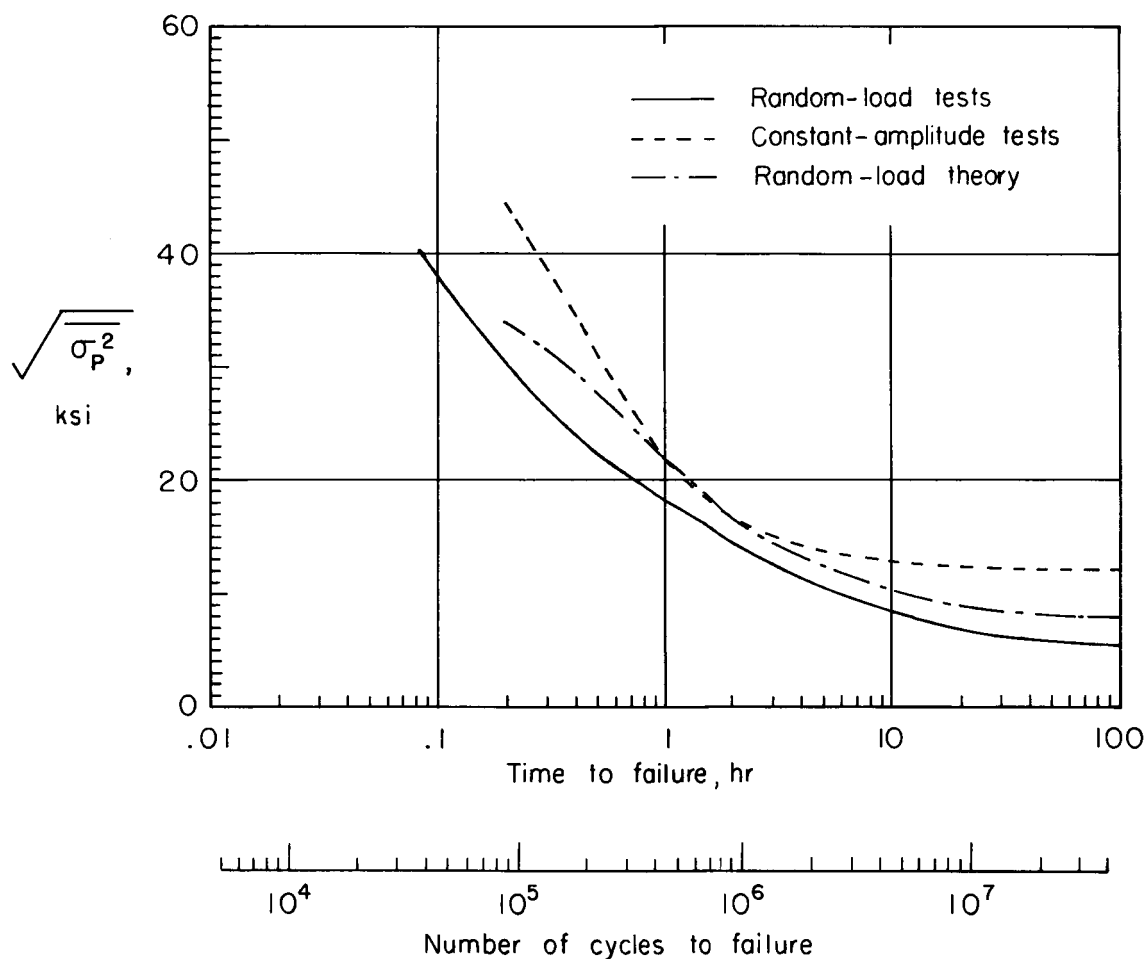


Figure 9.- Comparison of fatigue results of random-loading tests with fatigue results of constant-amplitude-loading tests and with theoretical results.  $\sqrt{\sigma_P^2}$  = Root-mean-square value of peak nominal stress.